

**DETERMINATION OF SUBSURFACE VELOCITY USING MULTICHANNEL  
ANALYSIS OF SURFACE WAVES**

**A DISSERTATION**

*Submitted in partial fulfillment of the*

*Requirements for the award of the degree*

*Of*

**INTEGRATED MASTER OF TECHNOLOGY**

*In*

**GEOPHYSICAL TECHNOLOGY**

**By**

**Shubham Kumar**



**DEPARTMENT OF EARTH SCIENCES**

**INDIAN INSTITUTE OF TECHNOLOGY ROORKEE**

**ROORKEE -247667(INDIA)**

**MAY, 2019**



**© INDIAN INSTITUTE OF TECHNOLOGY ROORKEE, 2019 ALL RIGHTS RESERVED**

## CANDIDATE'S DECLARATION

---

I Hereby announce that the work that is shown in this dissertation, titled “**DETERMINATION OF SUBSURFACE VELOCITY USING MULTICHANNEL ANALYSIS OF SURFACE WAVES**” in partial fulfillment of the requirement for the award of the degree of **INTEGRATED MASTER OF TECHNOLOGY** in **GEOPHYSICAL TECHNOLOGY** submitted to Department of Earth Sciences, Indian Institute of Technology, Roorkee carried out during May 2018- May 2019 is an original record of my own work done under the supervision of **Dr. Anand Joshi**, Professor, Indian Institute of Technology, Roorkee.

This matter incorporated in this dissertation has not been submitted by me for the award of any other degree or diploma of this Institute or any other university/Institute.


Date: May, 2019

Shubham Kumar  
Integrated M.Tech  
Final Year Geophysical  
Technology  
Department of Earth Sciences  
IIT Roorkee

## Certificate

---

This is to certify the work displayed in this thesis titled “**DETERMINATION OF SUBSURFACE VELOCITY USING MULTICHANNEL ANALYSIS OF SURFACE WAVES**” submitted by **Mr. Shubham Kumar** to Indian Institute of Technology, Roorkee in partial fulfillment of the requirements for the award of the degree is a record of original bona fide work of **INTEGRATED MASTER OF TECHNOLOGY** in **GEOPHYSICAL TECHNOLOGY** carried out by him with my guidance in the academic year 2018-2019.



**Dr. Anand Joshi**  
(Supervisor)  
Professor  
Department of Earth Sciences  
Indian institute of Technology, Roorkee  
Roorkee-India

## ACKNOWLEDGEMENT

---

*I convey my heartfelt gratitude to **Dr. Anand Joshi**, Professor, Indian Institute of Technology, Roorkee for his persistent support, motivation and inspiration throughout my dissertation work, deprived of which this would not have been possible. It was a privilege and an enlightening experience to work with him. I learnt a lot from him throughout my project work.*

*I am highly grateful to **Dr. Sunil Bajpai**, Head of Department of Earth Sciences, Department of Earth Sciences, IIT Roorkee, for helping me with all the required equipment and administrative support needed for the fulfillment of this work.*

*I am also thankful to all my friends, research scholars and non-teaching staffs for their great support throughout project work. A special mention to Rajat Mudgal for brainstorming sessions to develop ideas in this thesis. I am thankful to my batch-mates for keeping my spirits high throughout dissertation work.*

*Finally, I express my gratitude to my parents and my family members. Their blessings, inspiration and motivation have always kept me motivated.*

Date: May 2019

**Shubham Kumar**

## Abstract

---

The estimation of the in-situ shear wave velocity is carried out using various geophysical and other engineering techniques and methods. In this project, Multichannel analysis of the subsurface waves has been used. The most extensively used technique by geophysicists and geotechnical engineers is Multichannel Analysis of Surface Wave (MASW). The major reason behind the widespread use of this particular method is being its simplicity in generating and propagating the surface wave energy, and also the use of MASW method reduces cultural noise, improves the ground surface conditions.

The study area mainly falls in the lesser Himalayan terrain constitutes well defined low linear ranges of Siwalik sediments and rocks of Frontal Fold belt and is characterized by strike ridges, dip slopes with steep obsequent scarps, rectangular to trellis drainage pattern controlled by bedding and joints.

The data acquisition for the multichannel analysis of surface waves has been carried out using the TROMINO. Grilla software has been used to analyze the obtained results.

There are two sites where the study has been done and the results obtained at site1: Donal Khad, a total of 3 distinct interval velocities for respective depths can be identified and are present up to depth of 30 m. The value for the  $V_s(0.0-30) = 448$  m/s and for the site2: Balaknath Temple also 3 distinct interval velocities for respective depths can be identified and are present up to depth of 30 m. The value for the  $V_s(0.0-30) = 495$  m/s .

# Contents

---

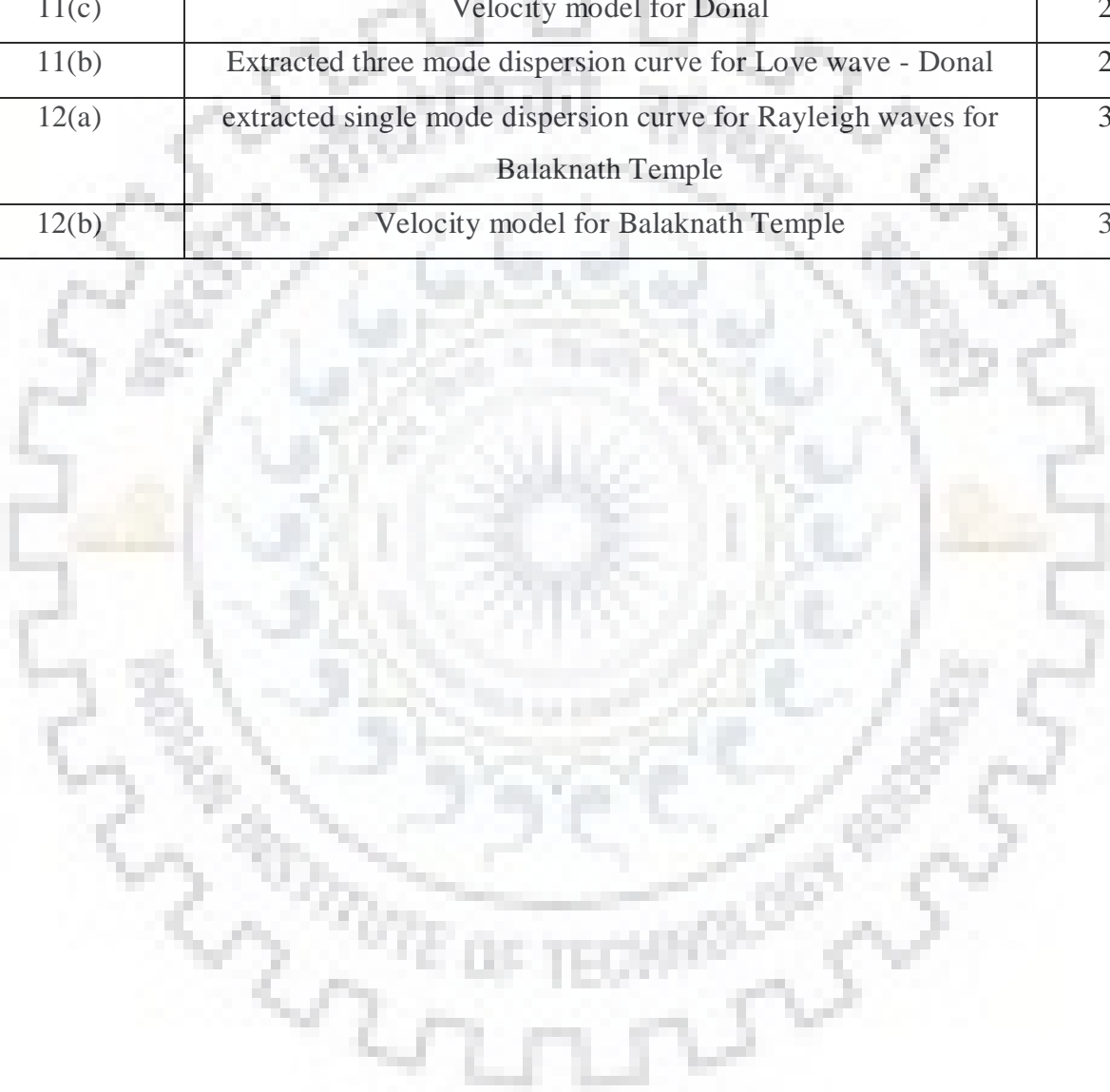
Topic	Page number
CANDIDATE'S DECLARATION .....	i
CERTIFICATE.....	ii
ACKNOWLEDGEMENT.....	iii
Abstarct .....	iv
List of Figures .....	vi
Chapter 1 - Introduction .....	1
Chapter 2: Theory .....	2
2.1 Dispersion Analysis .....	2
2.2 Horizontal to vertical spectral ratio (HVSR).....	6
Chapter 3: Geological settings of the study area .....	12
Chapter 4: Methodology.....	16
4.1 Data Acquisitions .....	16
4.2 Data Processing .....	22
Chapter 5: Results.....	29
Chapter 6: Conclusion.....	32
Chapter 7: References .....	33

## List of Figures

Fig. number	Description	Page number
1 (a)	Example of active recording	3
1(b)	Example of passive recording	3
1(c)	Typical dispersion curve, source	4
1(d)	Typical phase velocity spectra – Vs 30	4
2	Example of phase velocity spectra achieved precisely at the same site, by the same array, at changed times	5
3(a)	Avg. and synthetic H/V	10
3(b)	Amplitude spectra	10
3(c)	Velocity phase spectra	11
4(a)	India earthquake zone map	13
4(b)	Areal map of the study area depicted in white rectangle	13
4(c)	(c) proposed survey line	14
5	Topo sheet no. 53 A/7/SE and 53 A/11/SW	15
6(a)	Tromino	17
6(b)	Wireless Trigger,	17
6(c)	Sledge Hammer and Iron Plate	18
6(d)	Measuring tape	18
7(a-f)	Images from the sites during the data acquisitions	21
8 (a)	Typical recorded data in Grilla	22
8(b)	Parameter setting window for a 1D array	23
8(c)	Polygon selection of the recorded signal	24
9(a)	Recorded data signal	25
9 (b)	Polygon selection for the recorded signal	26
9(c)	Setting up the parameters	26



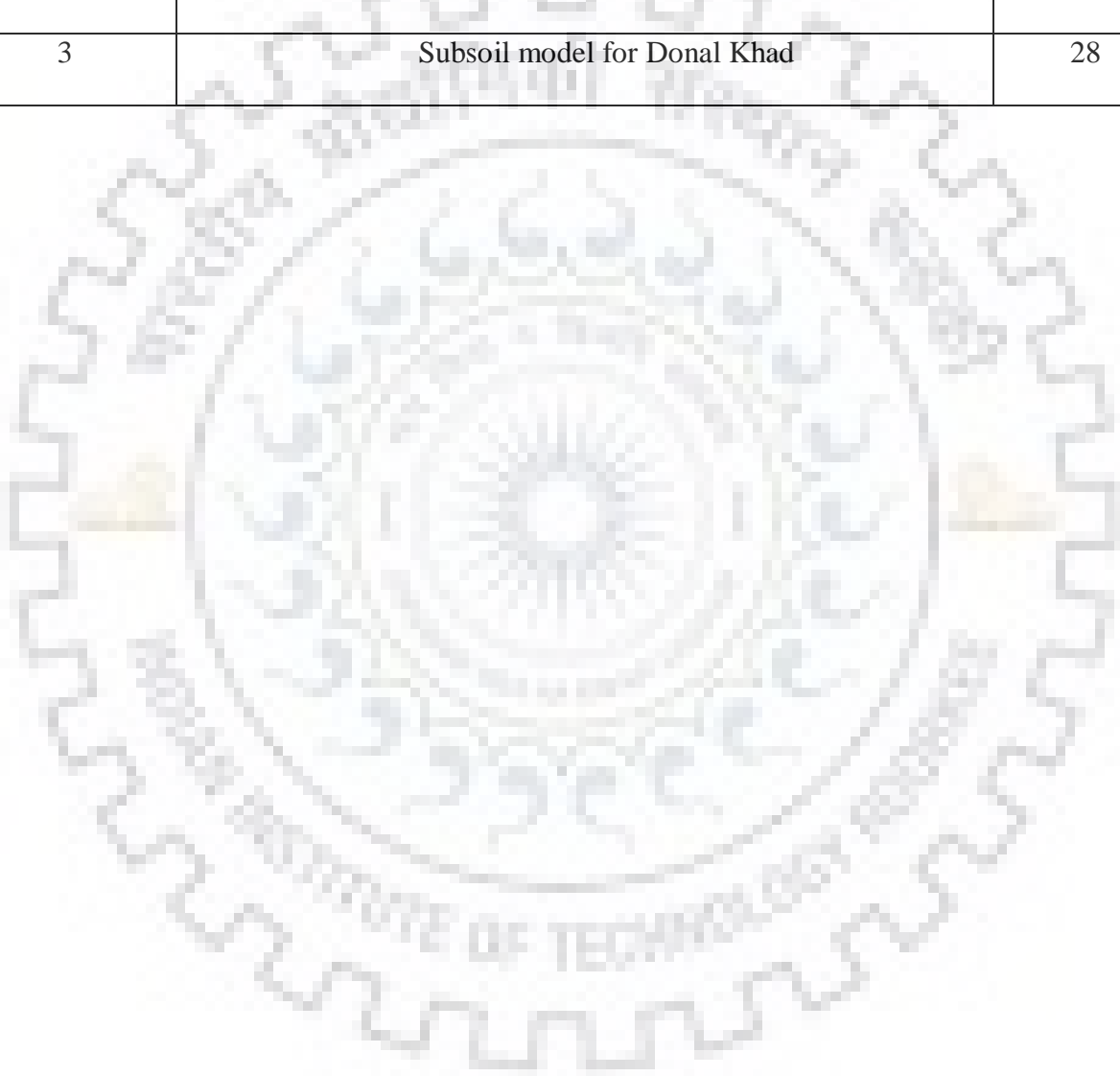
9(d)	velocity spectrum for the Donal site	27
10(a)	extracted dispersion curve after forward model obtained	27
10(b)	velocity depth model for Donal Khad	28
11(a)	extracted dispersion curve in single mode for Rayleigh Wave - Donal	29
11(c)	Velocity model for Donal	29
11(b)	Extracted three mode dispersion curve for Love wave - Donal	29
12(a)	extracted single mode dispersion curve for Rayleigh waves for Balaknath Temple	30
12(b)	Velocity model for Balaknath Temple	30



## List of Tables

---

Table no.	Description	Page no.
1	Example of input table. Note the 0 thickness (which actually means $\infty$ ) of the last layer and the empty $V_p$ column which will be filled automatically.	8
2	Typical Poisson's ratio values	9
3	Subsoil model for Donal Khad	28

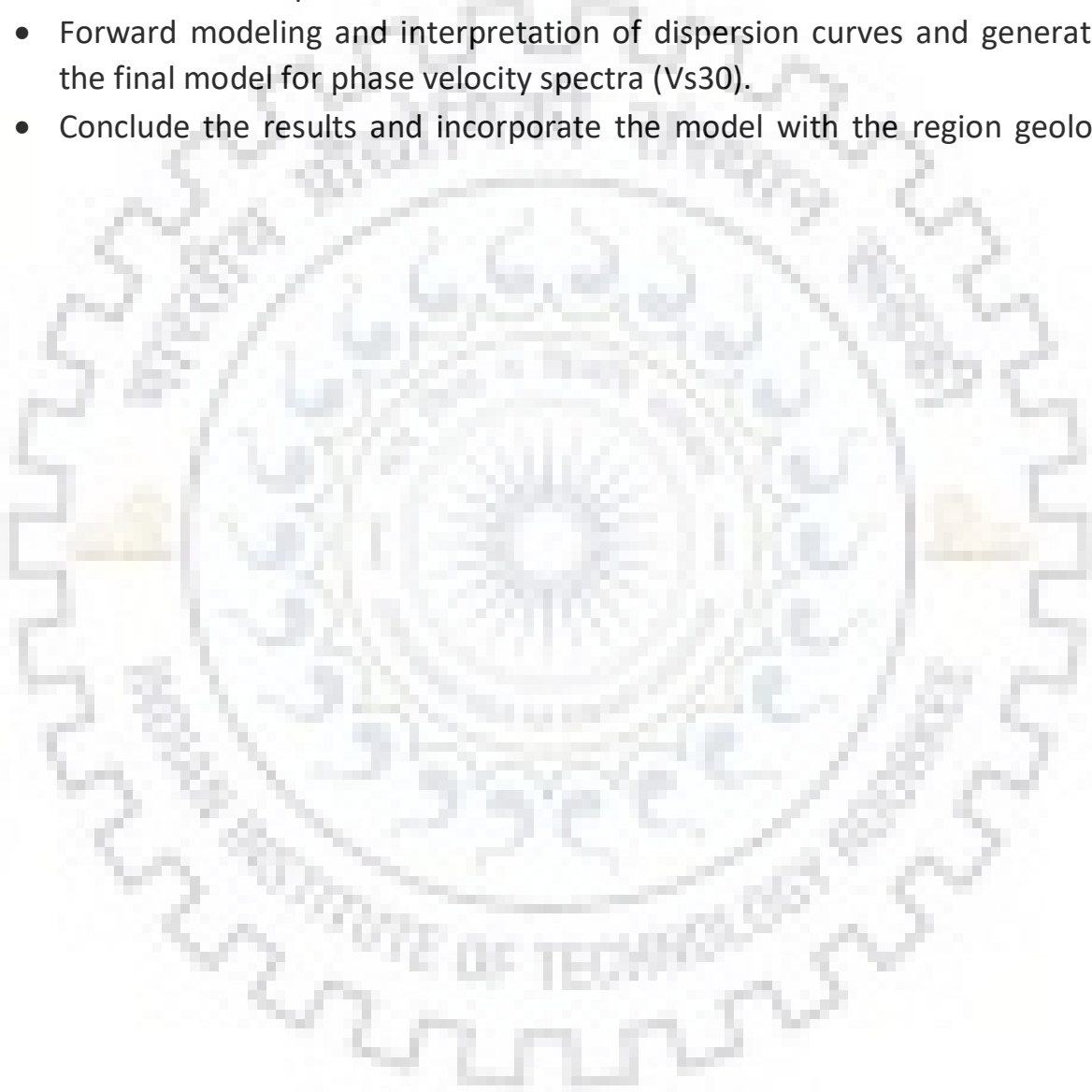


## Objective

---

Main objective of my dissertation work was to

- Visit the proposed site of abutments for the bridge. Acquisition of MASW data with the help of TROMINO.
- Simulation of dispersion curves.
- Forward modeling and interpretation of dispersion curves and generating the final model for phase velocity spectra ( $V_s30$ ).
- Conclude the results and incorporate the model with the region geology.



## Chapter 1 - Introduction

---

In various regions, the variable properties of the subsurface influence the most responses in various manners as the responds to the tremor produced by the earthquake ground motion.

The major subsoil parameters that hold a direct relationship with measureable parameter are stiffness of the soil, subsoil amplification ability and liquefaction. These parameters are directly related to the maximum capacity of the geotechnical structures they can especially in those regions which are seismically active zones and also used to map the geology of the subsurface structures. The major insights regarding the ground motion responses are estimated with the help of shear-wave velocity average over the first thirty meters.

The estimation of the in-situ shear wave velocity is carried out using various geophysical and other engineering techniques and methods. For example, estimation of shear wave velocity using the reflection and refraction methods and measuring the variations along continuous two dimension profiles. There are also other methods which aim to estimate shear wave velocity dissimilarities with depth at one surface location and results in a one-dimension velocity-depth model. These one-dimension velocity-depth model methods comprise borehole, suspension Primary-Secondary logger, and spectral analysis of surface waves (SASW), and majorly multichannel analysis of surface wave (MASW).

The most extensively used technique by geophysicists and geotechnical engineers is Multichannel Analysis of Surface Wave (MASW). The major reason behind the widespread use of this particular method is being its simplicity in generating and propagating the surface wave energy, and also the use of MASW method reduces cultural noise, improves the ground surface conditions and, quick acquisition of data on the fields and least ensuing processing (Miller et al., 2001).

## Chapter 2: Theory

---

### 2.1 Dispersion Analysis:

The variation of phase velocity with their frequencies is called dispersion, hence, their amplitude changes with depth. Surface waves of different wavelengths travels the subsurface layers at different depths and travel with the explicit velocity which describes the subsoil at the different depths. Surface waves that have a lower wavelength generally transmit slowly, while on the other hand waves with larger wavelength values travel faster. This property of surface waves, called dispersion. This particular property applies only to surface waves, such as Rayleigh and Love waves in layered media.

The techniques for retrieving dispersion curves from active fig.no.1 (a) or passive sources fig.no. 1(b) at two or more receivers has a variety of names concerning minor details regarding the geometry, source, etc. The main active methods include: SASW, spectral analysis of surface waves (Heisey et al., 1982; Nazarian and Stokoe, 1984); MASW, multichannel analysis of surface waves (Park et al., 1999), while the main passive methods are: SPAC, spatial autocorrelation Aki, 1957); ESAC extended spatial autocorrelation (Ohori et al., 2002); Re MiTM, Refraction MicrotemorTM (Louie, 2001); SSAP, statistical self-alignment property (Mulargia and Castellaro, 2013). The basis of all of all these active method techniques is being the slant stack (or the correlation) of the signal recorded from different receivers, that allows the determination of the propagation velocity of the surface waves of different frequencies that travels between layers.

The acquisition of the seismic signal is recorded at different positions depending on the site depictions (a minimum of two) over time using Radio transmitter and the phase velocity spectra using Grilla software are processed by slant stack and fast Fourier transform (FFT) procedures, which provide the most feasible velocity of the surveyed surface waves at each frequency.

Through this, a forward or inverse modeling procedure can be utilized which can help us out in generating the phase velocity model for the subsurface. The velocity spectra ( $V_s$ ) are linked to surface waves R or L (normally 10%– 15% larger) through the Poisson's ratio, as formulated in the elastic theory of waves.

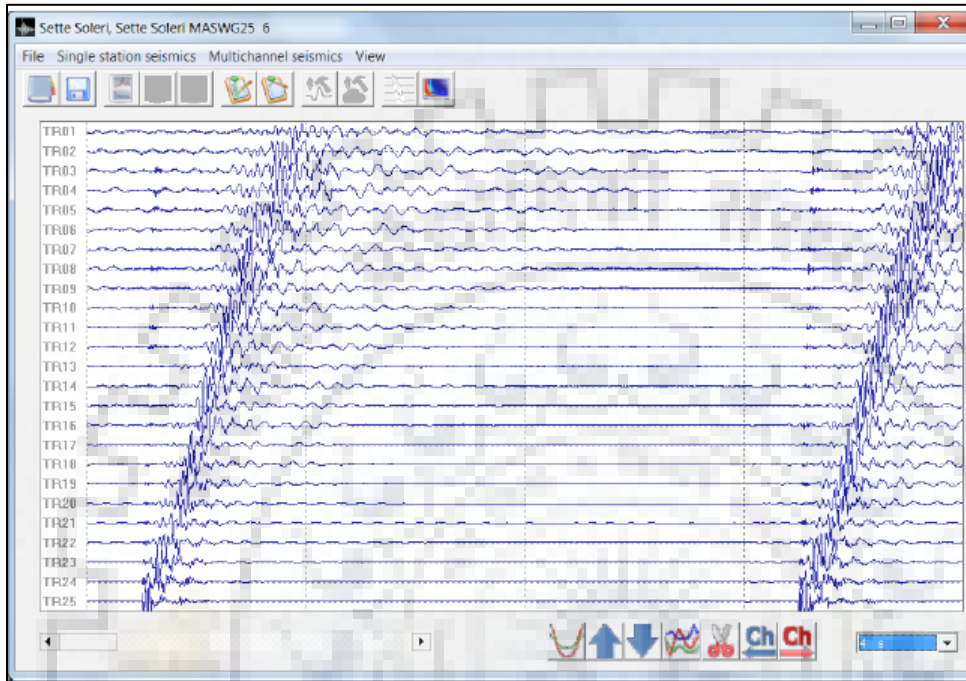


Fig. no. 1 (a) Example of active recording (source - <https://urlzs.com/nFxp>)

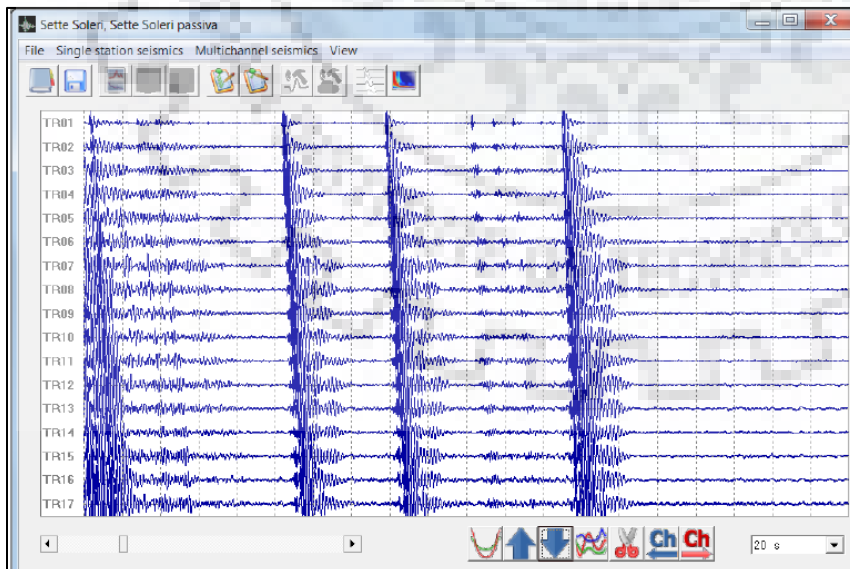


Fig.no. 1 (b) Example of passive recording, source - <https://urlzs.com/nFxp>

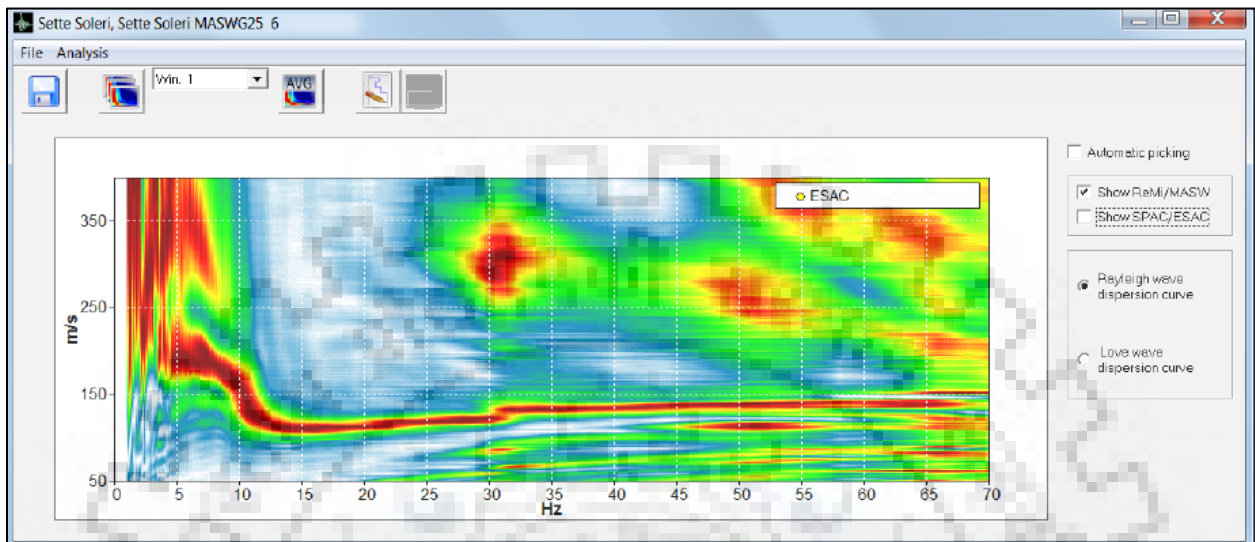


Fig. no. 1(c) Typical dispersion curve, source - <https://urlzs.com/nFxp>

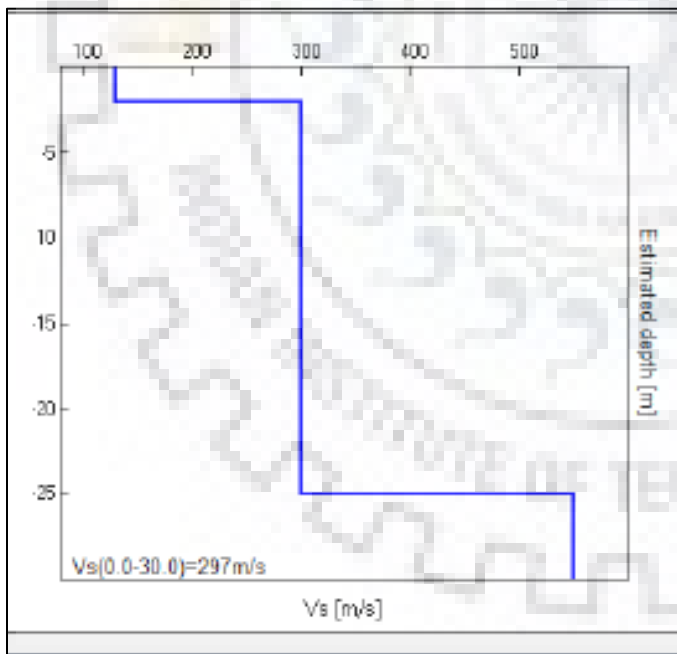


Fig. no. 1(d) typical phase velocity spectra – Vs 30, source - <https://urlzs.com/nFxp>

## Challenges: Interpretational Issues in dispersion analysis

- Unparalleled subsurface plane beneath the arrays at the survey site.
- Difference in the modeled dispersion curve fig. no. 2 on same survey area when the origin is reversed while surveying. Possible reasons might be due to – subsurface layers heterogeneity below the array and, due to the differences in source i.e. source variation.
- Non visibility of the fundamental mode in the dispersion curve.

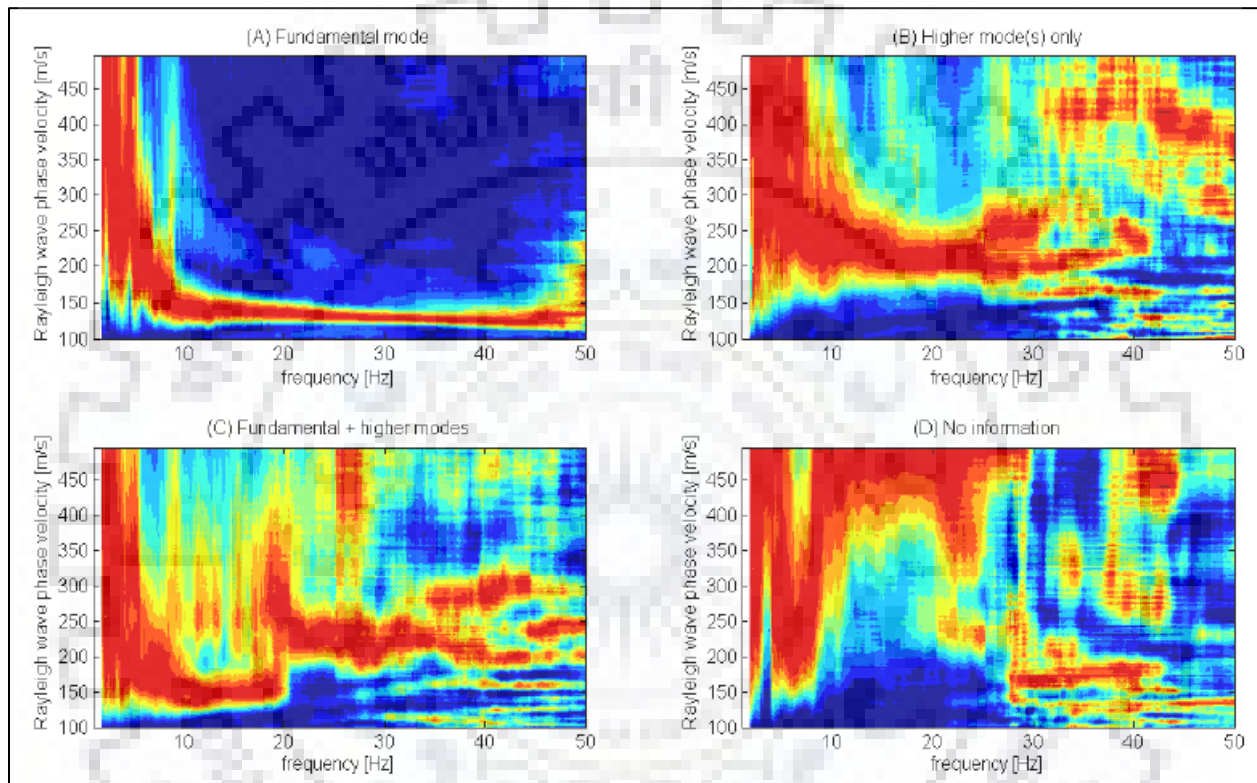


Fig. no. 2(Example of phase velocity spectra achieved precisely at the same site, by the same array, at changed times. Only different signal sources may be responsible for the different observed dispersion curves, source - <https://urlzs.com/nFx>)

A resolved prediction can be made for these problems with the aid of taking H/V curves along the array line.



## 2.2 Horizontal to vertical spectral ratio (HVSr)

The Horizontal to Vertical Spectral Ratio technique is a passive method, used widespread as a technique for studying the ground response, amplitude amplification of ground motion, which deals with the ambient seismic noise. The sources which produces micro tremors, like wind and onshore ocean currents contradicts in what is suggested to be the shear waves close to the surface (Yamanaka et al, 1994). The purpose of this particular method is to determine the seismic breaks and non-homogeneity of the surveyed bedrock layers using a technique about the spectral ratio Horizontal/Vertical, which is applied to a wide range of ground motion amplitude, from microtremor to strong motion. Nakamura (1989).

Wherever possible, the wave propagation is also aided by the means of men made activities, and these tremors are typically at lower wavelengths when comparison to waves generated by natural sources. This particular method factually describes that the constructive interference of waves in between a layer will create improved horizontal oscillations as compared to the vertical oscillations. A frequency spike which is related to the resonant frequency of the layer will be produced with the ratio of the horizontal and vertical components. (Ali, Moro, 2015).

Generally, in cases when we have an ideal condition having 2 layers earth model, estimation of the shear wave velocity( $V_s$ , in m/s) for the top most layer can be done with the aid of the peak fundamental frequency of the top layer if the two layers show a great enough impedance difference (Mucciarelli, 2001, Di Stefano et al, 2014).

The acquirement of the spectral ratio of horizontal and vertical is fast and useful and also there is no any necessity of cable array. The non-requirement of any energy source in this method, it becomes a passive technique. The source for the seismic tremors is natural noises.

Horizontal to vertical spectral ratio technique for stratigraphic purposes can be employed:

- i) As a preliminary surveying technique for locating the sites on which investigation is possible with the classical techniques,
- ii) To verify, when other data already exist, the presence of significant heterogeneities around the sites investigated,

iii) As an element to supplement other investigations

The characteristic conclusions that can be obtained from HVSR:

- The distinctive resonance frequency of the survey area.
- Fundamental resonating frequency
- The average  $V_s$  and thickness of the imposed bedrock.

Several H/V curves acquired along the proposed array on the sites using TROMINO. The H/V curves are converted from the frequency to the depth domain by using the  $V_s$  profile derived from the joint fit of the single- station and array curves, as in Amorosi et al. (2008). Alternatively, they can be converted to the depth domain by using the initial  $V_s$  model suggested from the array or other constraints and using simplified  $V_s$ -depth relations as in Ibs-von Seht and Wohlenberg (1999). In the resulting contour plot, the H/V peaks have been migrated to the depth domain, thus indicating the location and disposition of the stiff layer(s).

Occam's Razor principle:

This means that among the many (or infinite) models that can equally reproduce the experimental data, the simplest model (i.e. the one with less parameter) should be used. The well-known equation

$$\lambda = v/f,$$

Wavelength = velocity / frequency helps us figuring out the size of the seismic reflectors needed to give some signal of their existence at each frequency. It also helps us focusing the attention on the main features of the H/V curve (i.e. the clear peaks 1 only) and to neglect the minor wiggles that can represent higher modes etc.

### **Input parameter in Grilla for HVSR**

The surface wave modeling in Grilla requires the following input parameters for each layers:

- Thickness of the layer in [m]
- $V_s$ , S-wave velocity in [m/s]
- Density in  $10^3 \text{ kg/m}^3$ .

The last layer of the model is assumed to have an infinite thickness. This must be indicated with 0 thicknesses.

The  $V_P$  column cannot be filled manually table no. 1. This is compiled automatically on the basis of the  $V_S$  and Poisson's ratio values inserted by the user manually.

Table 1: Example of input table. Note the 0 thickness (which actually means  $\infty$ ) of the last layer and the empty  $V_P$  column which will be filled automatically.

S.No	Thickness (m)	$V_P$ (m/s)	$V_S$ (m/s)	U Poiss.	Density ( $10^3$ )
1	10		220	0.4	1.7
2	30		300	0.4	1.8
3	0		450	0.4	2.0

$V_P$  and density do not play a relevant role in any surface wave-based technique. This implies that the theoretical H/V shape is primarily affected by the  $V_S$  profile only.

**ANY SURFACE WAVE-BASED MODEL DO NOT PROVIDE  $V_P$  AND DENSITY PROFILES**

Typically, densities in the range 1.6-2.2  $10^3$  kg/m<sup>3</sup> and  $V_P$  depending on  $V_S$  according to the Poisson's ratio

$$U = (V_P^2 - 2V_S^2) / [2(V_P^2 - V_S^2)]$$

This will be used in natural materials, being  $V_P > V_S$ , the Poisson's ratio is included in the [0, 0.5] interval and in the shallow subsoils it varies between 0.38 and 0.49.

The Poisson's ratio estimated through geophysical prospections in the field is usually much larger than the same modulus calculated at the sample scale in the laboratory. The sample size involved in the geophysical prospectation is much larger and at this scale the sample is usually layered, fractured etc. This lowers seismic wave velocities and their ratios considerably in the field, compared to the 'ideal' sample of the laboratory.

Note that in soft soils (i.e. soils that would present  $V_p < \approx 1450$  m/s in dry conditions) under the water table, the P wave transmits through the fluid phase with a velocity  $V_p \approx 1450$  m/s. The Poisson's ratio must therefore be chosen in order to get  $V_p \approx 1450$  m/s from the VS velocity estimated for that site/layer.

There might be the cases when no independent measurements of the Poisson's ratio are available, in such cases values in the given below Table no. 2 are considered

Table 2: Typical poisson's ratio values

<b>Material</b>	<b>Typical U</b>
Hard Rock	0.35
Soft- Rock	0.38
Sand - Gravel	0.4-0.42
Clay	0.45-0.48
Soft-soil ( $V_p \leq 1450$ m/s in dry cond.)under water	U to be chosen so that $V_p = 1450$ m/s

For a single layer of thickness H overlying the bedrock, from the resonance equation, we have

$$F_0 = V_s / (4H)$$

It is stress-free to understand that a H/V curve – which provides  $F_0$  only – leaves the equation underdetermined. So, in order to estimates  $V_s$ , it is compulsory to know H or vice versa.

In order to obtain  $V_s$  profile from an H/V curve, constraints must be declared. With no constraint, infinite solutions can be obtained.

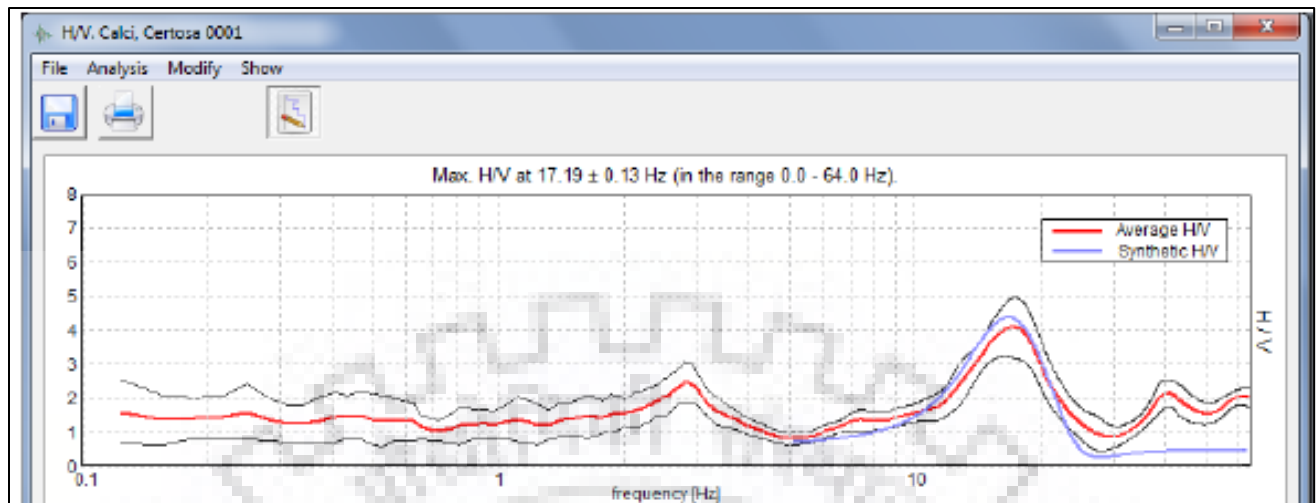


Fig. no. 3 (a)

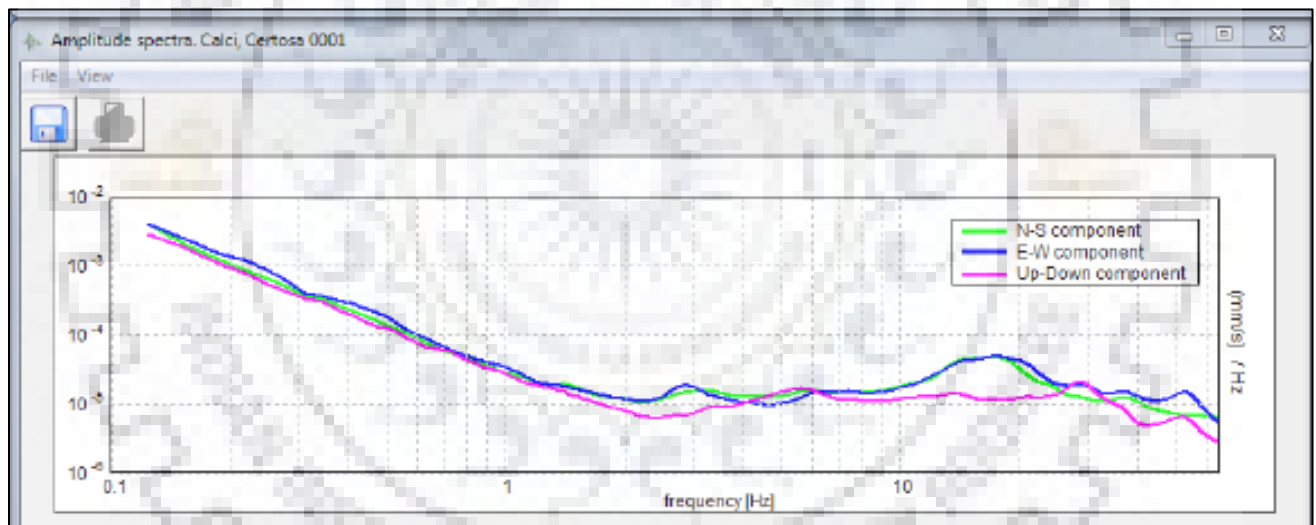


Fig. no. 3 (b)

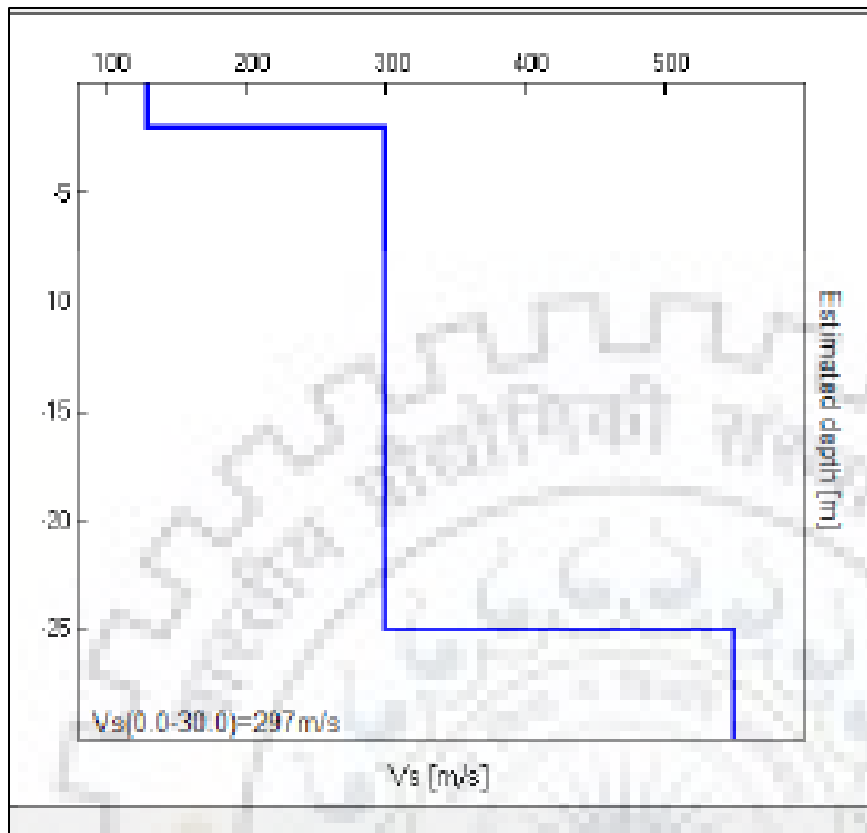


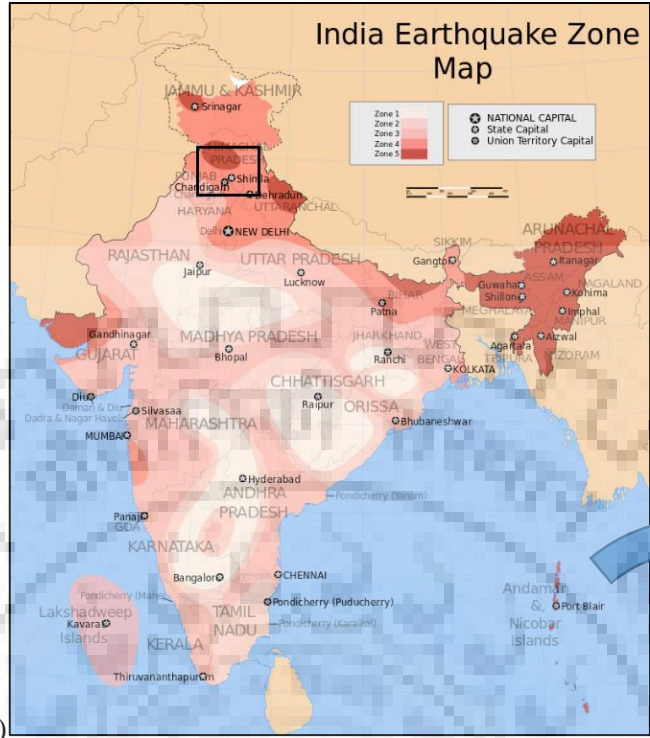
Fig. no. 3(c)

Fig.no. 3 (a) Avg. and synthetic H/V (b) Amplitude spectra (c) Velocity phase spectra (Image Source - (source - <https://urlzs.com/nFxp>)TROMINO® user manual)

### Chapter 3: Geological settings of the study area

---

The study area fig. no. 4(b) and 4(c) mainly falls in the lesser Himalayan terrain constitutes well defined low linear ranges of Siwalik sediments and rocks of Frontal Fold belt and is characterized by strike ridges, dip slopes with steep obsequent scarps, rectangular to trellis drainage pattern controlled by bedding and joints. The proposed 20 km long section of Bhanupali – Bilaspur – Beri Rail link project section take off from Bhanupali at km 0.002 and passing through the older alluvium represented by clay with calcrete nodules, silt and sand of Ludhiana Formation up to km 3.800. From km 3.800 to km 12.200, the alignment is passing through rocks belonging to Upper Siwalik Group represented by soft sandstone; siltstone, boulder beds and a coarse sandstone/Conglomerate band of retracted. The general trend of the rock mass as observed in the area is  $N45^{\circ} W - S45^{\circ} E$  and dip varying from  $75^{\circ}$  to over  $85^{\circ}$  south westerly. Between chainage km 12.200 and km 18.000 the alignment passes through rocks belonging to Middle Siwalik Group represented by grayish and brownish nodular sandstone and claystone bands of variable thickness. The general trend of the rock mass is NW-SE with dip varying from  $55^{\circ}$  to over  $75^{\circ}$  South Westerly. From chainage km 18.000 to km19.000, the alignment enters into rocks belonging to lower Siwalik Group represented by comparatively compact bands of sandstone with alternate bands of claystone and sandy clay. The general trend of the rock unit is NW-SE dip vary from  $55^{\circ}$  to over  $75^{\circ}$  Northeasterly. Besides these, rock units are also traversed by number of joint sets, where bedding joint is bedding joint is the prominent joint set. In general the Siwalik rocks are weak to very weak in nature and classified as poor to very quality of the rock mass.



4 (a)



4(b)





4(c)

Fig. no. 4 - (a) India earthquake zone map (source- Wikipedia), (b) areal map of the study area depicted in white rectangle (source – Google map), (c) proposed survey line (source – <https://urlzs.com/yDiH>: RVNL report)

The study area falls on the Survey of India topo sheet No. 53 A/7/SE and 53 A/11/SW fig. no. 5 on 1:15000 scale. The present alignment passes through Punjab and in the part of Himachal Pradesh.

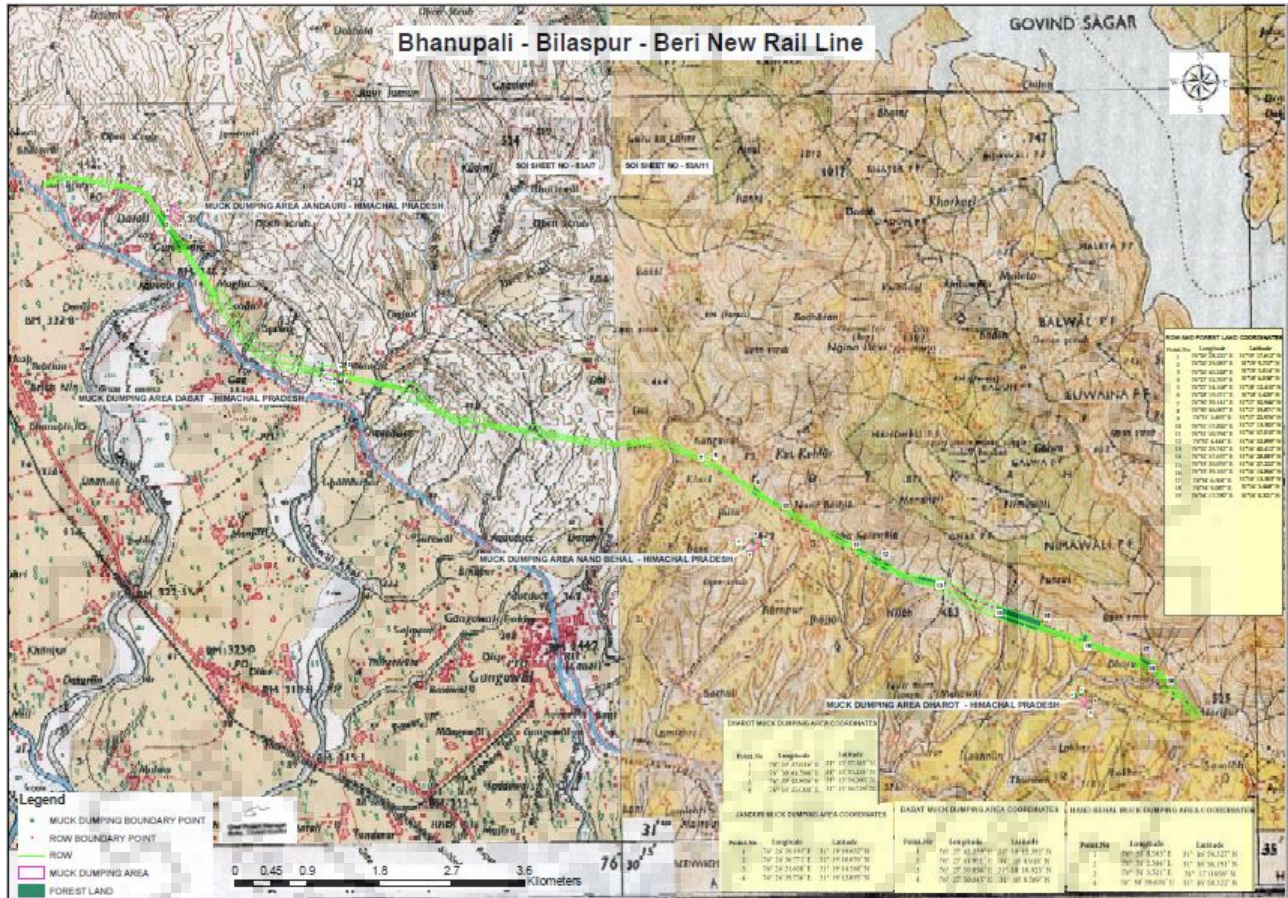


Fig. no. 5 Topo sheet no. 53 A/7/SE and 53 A/11/SW on 1:15000 scales.

(Source- <https://urlzs.com/yDiH>)

## Chapter 4: Methodology

---

### 4.1 Data Acquisitions

- Instruments

For the data acquisition part TROMINO® fig. no. 6(a) is used with a wireless trigger fig.no. 6(b) that comes along with the TROMINO® and the wireless trigger is used only for MASW.

Choosing TROMINO® over other traditional MASW analysis instruments provides an edge in various ways. It provides a high-resolution result for both passive and active seismic surveys and tremor observing. This equipment has following components:

- Two velocity measuring for seismic ambient micro tremor and strong motion data recordings
- Three acceleration measuring channels for strong tremor recording, one analog channel
- A Global Positioning System receiver.
- Antenna for the positioning and complete synchronization among various parts.

A continuous mode with no any time-limits or user defined time intervals modes can be used while recording in Tromino. The main purpose for designing the Tromino was particularly measure the subsoil characterization more accurately with minimal efforts.



6(a) Tromino



6(b)



6(c)



6(d)

Fig.no.6 (a) Tromino (b) Wireless Trigger, (c) Sledge Hammer and Iron Plate and, (d) measuring tape (Source – personal camera)

## Wireless Trigger (WT)

The Wireless Trigger (WT) fig. no 6(b) a radio device that transmits an impulse to **TROMINO®** when a threshold level is passed in the built-in tri-axial accelerometer, in an external geophone or other device connected to the WT.

Two parameters need to be defined: 1) the threshold measurement device (internal accelerometer, external geophone/other), 2) the trigger level (low, medium, high).

The WT is used to mark the origin time in the multichannel seismic techniques based on both body and surface waves (e.g. seismic refraction, MASW with Rayleigh and Love waves). By keeping the receiver (**TROMINO®**) at a fixed position and by moving the source and the WT at different offsets from **TROMINO®**, the *Grilla* software will automatically merge the recordings in a 3-D multichannel recording.

Sledge hammers (20 lbs) and iron plate fig. no 6 (c) were used to generate the seismic signal and 2 measuring tapes fig. no. 6(d).

The data acquisition part was carried out at 2 proposed sites for the abatement of bridge.

- Site 1: Donal Khad
- Site 2: Balaknath Temple

Below here are some of the images captured during the data acquisition on different sites:



Fig. no. 7(a)



Fig. no. 7(b)



Fig. no. 7(c)



Fig. no. 7(d)



Fig. no. 7(e)



Fig. no. 7(f)

Fig. no. 7(a-f) images from the sites during the data acquisitions



## 4.2 Data Processing

For the processing of the acquired data *Grilla software* is used. Procedure for the data processing is carried out in the following manner:

- (a) Open dispersion curve module in *Grilla software*
- (b) Setting up the required parameters (min. & max. frequency, min. & max. velocity, window length, array geometry – X(m), Y(m))
- (c) Polygon selection of the recorded signal.
- (d) Create dispersion curve
- (e) Forward modeling of dispersion curve to obtain the phase velocity spectra.

The settings for the Grilla software:

Site	Trace	Serial no.	Day	Start	End	Length	Hz [Hz]	GPS	Doc.
1	Dharoi Bridge 1 Abutment A1	[EW] Tromino at A MASW	SSR-PSEUDO	26/02/18	14:58:18	15:03:28	0' 2"	512	
2	Dharoi Bridge 1 Abutment A1	[EW] Tromino at B MASW	SSR-PSEUDO	26/02/18	15:08:04	15:17:36	0' 2"	512	
3	Dharoi Bridge 1 Abutment A1	[NS] Tromino at A MASW	SSR-PSEUDO	26/02/18	14:54:18	15:03:28	0' 2"	512	
4	Dharoi Bridge 1 Abutment A1	[NS] Tromino at B MASW	SSR-PSEUDO	26/02/18	15:08:04	15:17:36	0' 2"	512	
5	Dharoi Bridge 1 Abutment A1	[E] Tromino at A MASW	SSR-PSEUDO	26/02/18	14:54:18	15:03:28	0' 2"	512	
6	Dharoi Bridge 1 Abutment A1	[E] Tromino at B MASW	SSR-PSEUDO	26/02/18	15:08:04	15:17:36	0' 2"	512	
7	Dharoi Bridge 1 Abutment A1	Tromino at A MASW	TE340294/01-17	26/02/18	14:54:18	15:03:28	9' 0"	TRC	512
8	Dharoi Bridge 1 Abutment A1	Tromino at B MASW	TE340294/01-17	26/02/18	15:08:04	15:17:36	9' 24"	TRC	512
9	Dharoi Bridge 1 Abutment A2	[EW] Tromino at A MASW	SSR-PSEUDO	26/02/18	10:44:32	10:52:08	0' 2"	512	
10	Dharoi Bridge 1 Abutment A2	[EW] Tromino at B MASW	SSR-PSEUDO	26/02/18	11:02:30	11:10:53	0' 2"	512	
11	Dharoi Bridge 1 Abutment A2	[NS] Tromino at A MASW	SSR-PSEUDO	26/02/18	10:44:32	10:52:08	0' 2"	512	
12	Dharoi Bridge 1 Abutment A2	[NS] Tromino at B MASW	SSR-PSEUDO	26/02/18	11:02:30	11:10:53	0' 2"	512	
13	Dharoi Bridge 1 Abutment A2	[E] Tromino at A MASW	SSR-PSEUDO	26/02/18	10:44:32	10:52:08	0' 2"	512	
14	Dharoi Bridge 1 Abutment A2	[E] Tromino at B MASW	SSR-PSEUDO	26/02/18	11:02:30	11:10:53	0' 2"	512	
15	Dharoi Bridge 1 Abutment A2	Tromino at A MASW	TE340294/01-17	26/02/18	10:44:32	10:52:08	7' 36"	TRC	512
16	Dharoi Bridge 1 Abutment A2	Tromino at B MASW	TE340294/01-17	26/02/18	11:02:30	11:10:53	8' 12"	TRC	512
17	Dharoi Bridge 2 Abutment A1	[EW] Tromino at A MASW	SSR-PSEUDO	26/02/18	12:18:04	12:28:12	0' 2"	512	
18	Dharoi Bridge 2 Abutment A1	[EW] Tromino at B MASW	SSR-PSEUDO	26/02/18	12:35:44	12:46:00	0' 2"	512	
19	Dharoi Bridge 2 Abutment A1	[NS] Tromino at A MASW	SSR-PSEUDO	26/02/18	12:18:04	12:28:12	0' 2"	512	
20	Dharoi Bridge 2 Abutment A1	[NS] Tromino at B MASW	SSR-PSEUDO	26/02/18	12:35:44	12:46:00	0' 2"	512	
21	Dharoi Bridge 2 Abutment A1	[E] Tromino at A MASW	SSR-PSEUDO	26/02/18	12:18:04	12:28:12	0' 2"	512	
22	Dharoi Bridge 2 Abutment A1	[E] Tromino at B MASW	SSR-PSEUDO	26/02/18	12:35:44	12:46:00	0' 2"	512	
23	Dharoi Bridge 2 Abutment A1	Tromino at A MASW	TE340294/01-17	26/02/18	12:18:04	12:28:12	10' 0"	TRC	512
24	Dharoi Bridge 2 Abutment A1	Tromino at B MASW	TE340294/01-17	26/02/18	12:35:44	12:46:00	10' 12"	TRC	512
25	Dharoi Bridge 2 Abutment A2	[EW] Tromino at A MASW	SSR-PSEUDO	26/02/18	13:42:11	13:51:41	0' 2"	512	
26	Dharoi Bridge 2 Abutment A2	[EW] Tromino at B MASW	SSR-PSEUDO	26/02/18	13:56:45	14:07:12	0' 2"	512	
27	Dharoi Bridge 2 Abutment A2	[NS] Tromino at A MASW	SSR-PSEUDO	26/02/18	13:42:11	13:51:41	0' 2"	512	
28	Dharoi Bridge 2 Abutment A2	[NS] Tromino at B MASW	SSR-PSEUDO	26/02/18	13:56:45	14:07:12	0' 2"	512	
29	Dharoi Bridge 2 Abutment A2	[E] Tromino at A MASW	SSR-PSEUDO	26/02/18	13:42:11	13:51:41	0' 2"	512	
30	Dharoi Bridge 2 Abutment A2	[E] Tromino at B MASW	SSR-PSEUDO	26/02/18	13:56:45	14:07:12	0' 2"	512	
31	Dharoi Bridge 2 Abutment A2	Tromino at A MASW	TE340294/01-17	26/02/18	13:42:11	13:51:41	9' 24"	TRC	512
32	Dharoi Bridge 2 Abutment A2	Tromino at B MASW	TE340294/01-17	26/02/18	13:56:45	14:07:12	10' 24"	TRC	512
33	Donsal Bridge Abutment A2	[EW] Tromino at A MASW	SSR-PSEUDO	26/02/18	17:16:09	17:31:42	0' 2"	512	
34	Donsal Bridge Abutment A2	[EW] Tromino at B MASW	SSR-PSEUDO	26/02/18	17:41:55	18:00:30	0' 2"	512	
35	Donsal Bridge Abutment A2	[NS] Tromino at A MASW	SSR-PSEUDO	26/02/18	17:16:09	17:31:42	0' 2"	512	
36	Donsal Bridge Abutment A2	[NS] Tromino at B MASW	SSR-PSEUDO	26/02/18	17:41:55	18:00:30	0' 2"	512	

Fig.no.8 (a) Typical recorded data in Grilla

In order to start with producing the phase velocity spectra – click on *the Open dispersion curve module button* from the trace toolbar. The response to this action will pop up a parameter setting window 8(a) and 7(b).

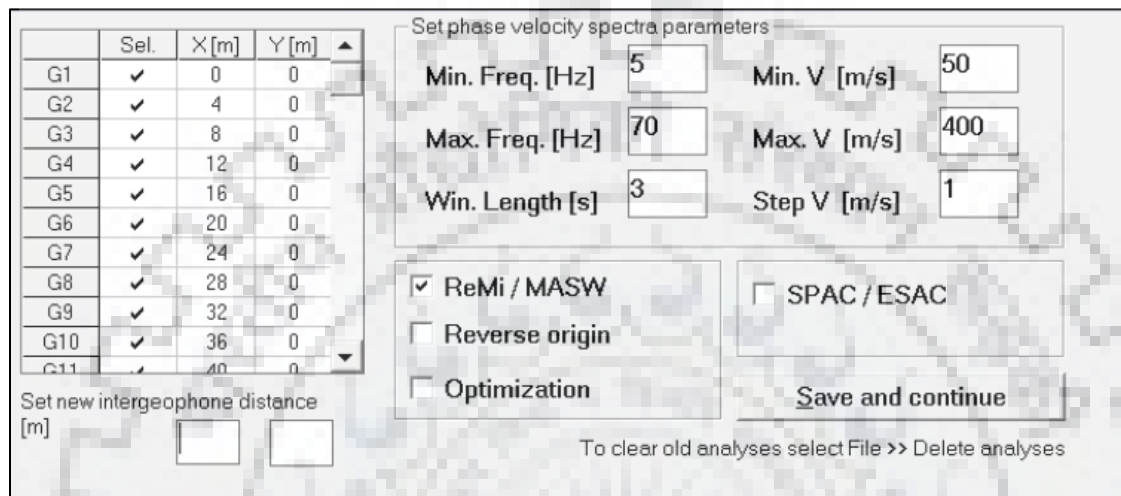


Fig.no. 8(b) (Parameter setting window for a 1D array)

User need to define the following parameters:

- 1) The active channels. If you wish to select all the channels, click the SEL. column header and to include/exclude channels click on the relative line.
- 2) The array geometry (X[m], and Y[m] columns). These values are actually the distance from the first geophone G1 of the array and must therefore be increasing in a linear array.
- 3) The parameters for the phase velocity spectra. These are the parameters to set in the frame Set phase velocity spectra parameters:
  - MIN. FREQ. [Hz] is the lower bound frequency of computation of the phase velocity spectra.
  - MAX. FREQ. [Hz] is the higher bound frequency of computation of the phase velocity spectra.
  - MIN. VEL. [m/s] is the lower bound velocity of computation of the phase velocity spectra ,

- MAX. VEL. [m/s] is the higher bound frequency of computation of phase velocity spectra ,
- STEP V. [m/s] is the Vs step of computation of the phase velocity spectra (this means that spectra will be computed from MIN. VEL. to MAX. VEL., step STEP V.)
- WIN. LENGTH [s] is the length in seconds of the windows on which the phase velocity spectra will be calculated. Example: if you set WIN. LENGTH. [s] = 10 and your recording lasted 5 minutes; you will get 30 phase velocity spectra.

The analysis of the recorded signal is more refined by selecting a polygon fig. no. 8(c) (only a specific part) as MULTICHANNEL SEISMICS > SURFACE WAVES > SELECT AREA and set the four vertices of the polygon to analyse.

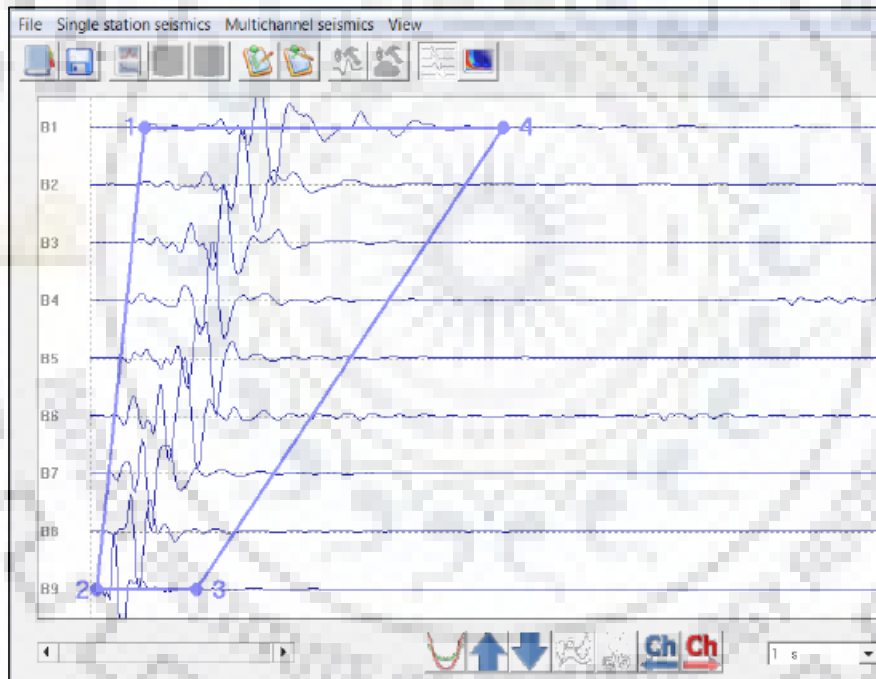


Fig. no. 8(c) (Polygon selection of the recorded signal)

After marking the selection points of the, the phase velocity spectra and the dispersion curve can be produced by clicking the right most dispersion curve icon on the tool bar.

Final process in the forward modeling of the dispersion curve to produce the velocity depth model.

The Forward modeling is carried out for the dispersion curve with the sole purpose of this particular process is to generate a velocity depth model with the help of velocity phase spectra and for these we need to get an idea about the maximum and minimum depth of investigation. For this, we need to calculate the maximum depth of investigation it is necessary to define the phase velocity at which the minimum frequency of the dispersion curve is defined.

Following steps are helpful in doing so:

- Figure out the fundamental frequency and the points on curve where the slope of dispersion curve changes (knee points) from right to left i.e. from higher frequency to lower frequency.
- For the first layer thickness, dividing the wavelength of first knee point by 2 or 3.
- Iterate the procedure with further knee points until you reach the maximum depth of investigation.
- Keeping in mind to adjust the modeling frequency intervals of the theoretical dispersion curve so that there can be a match between the actual experimental dispersion curves.

Data processing of the sites.

Site 1: Donal Khad

- Recorded data signal in Grilla

Site	Layer	Sensor	Type	Date	Start	End	Length	Fr. Vel.	LPS	Log
1	Dhawal Bridge 1 Abutment A1	[E]V1 Torsion at A MAS5v	SSR-PSEUDO	26/02/18	14:54:18	15:03:28	0' 2"	512		
2	Dhawal Bridge 1 Abutment A1	[E]V1 Torsion at B MAS5v	SSR-PSEUDO	26/02/18	15:08:04	15:17:36	0' 2"	512		
3	Dhawal Bridge 1 Abutment A1	[N5] Torsion at A MAS5v	SSR-PSEUDO	26/02/18	14:54:18	15:03:28	0' 2"	512		
4	Dhawal Bridge 1 Abutment A1	[N5] Torsion at B MAS5v	SSR-PSEUDO	26/02/18	15:08:04	15:17:36	0' 2"	512		
5	Dhawal Bridge 1 Abutment A1	[C2] Torsion at A MAS5v	SSR-PSEUDO	26/02/18	14:54:18	15:03:28	0' 2"	512		
6	Dhawal Bridge 1 Abutment A1	[C2] Torsion at B MAS5v	SSR-PSEUDO	26/02/18	15:08:04	15:17:36	0' 2"	512		
7	Dhawal Bridge 1 Abutment A1	Torsion at A MAS5v	TE3GCM49-17	26/02/18	14:54:18	15:03:28	9' 0"	19C		
8	Dhawal Bridge 1 Abutment A1	Torsion at B MAS5v	TE3GCM49-17	26/02/18	15:08:04	15:17:36	9' 24"	19C		
9	Dhawal Bridge 1 Abutment A2	[E]V1 Torsion at A MAS5v	SSR-PSEUDO	26/02/18	10:44:32	10:52:08	0' 2"	512		
10	Dhawal Bridge 1 Abutment A2	[E]V1 Torsion at B MAS5v	SSR-PSEUDO	26/02/18	11:02:36	11:10:53	0' 2"	512		
11	Dhawal Bridge 1 Abutment A2	[N5] Torsion at A MAS5v	SSR-PSEUDO	26/02/18	10:44:32	10:52:08	0' 2"	512		
12	Dhawal Bridge 1 Abutment A2	[N5] Torsion at B MAS5v	SSR-PSEUDO	26/02/18	11:02:36	11:10:53	0' 2"	512		
13	Dhawal Bridge 1 Abutment A2	[C2] Torsion at A MAS5v	SSR-PSEUDO	26/02/18	10:44:32	10:52:08	0' 2"	512		
14	Dhawal Bridge 1 Abutment A2	[C2] Torsion at B MAS5v	SSR-PSEUDO	26/02/18	11:02:36	11:10:53	0' 2"	512		
15	Dhawal Bridge 1 Abutment A2	Torsion at A MAS5v	TE3GCM49-17	26/02/18	10:44:32	10:52:08	7' 30"	19C		
16	Dhawal Bridge 1 Abutment A2	Torsion at B MAS5v	TE3GCM49-17	26/02/18	11:02:36	11:10:53	8' 12"	19C		
17	Dhawal Bridge 2 Abutment A1	[E]V1 Torsion at A MAS5v	SSR-PSEUDO	26/02/18	12:19:04	12:28:12	0' 2"	512		
18	Dhawal Bridge 2 Abutment A1	[E]V1 Torsion at B MAS5v	SSR-PSEUDO	26/02/18	12:25:44	12:46:08	0' 2"	512		
19	Dhawal Bridge 2 Abutment A1	[N5] Torsion at A MAS5v	SSR-PSEUDO	26/02/18	12:19:04	12:28:12	0' 2"	512		
20	Dhawal Bridge 2 Abutment A1	[N5] Torsion at B MAS5v	SSR-PSEUDO	26/02/18	12:25:44	12:46:08	0' 2"	512		
21	Dhawal Bridge 2 Abutment A1	[C2] Torsion at A MAS5v	SSR-PSEUDO	26/02/18	12:19:04	12:28:12	0' 2"	512		
22	Dhawal Bridge 2 Abutment A1	[C2] Torsion at B MAS5v	SSR-PSEUDO	26/02/18	12:25:44	12:46:08	0' 2"	512		
23	Dhawal Bridge 2 Abutment A1	Torsion at A MAS5v	TE3GCM49-17	26/02/18	12:19:04	12:28:12	10' 0"	19C		
24	Dhawal Bridge 2 Abutment A1	Torsion at B MAS5v	TE3GCM49-17	26/02/18	12:25:44	12:46:08	10' 12"	19C		
25	Dhawal Bridge 2 Abutment A2	[E]V1 Torsion at A MAS5v	SSR-PSEUDO	26/02/18	13:42:11	13:51:41	0' 2"	512		
26	Dhawal Bridge 2 Abutment A2	[E]V1 Torsion at B MAS5v	SSR-PSEUDO	26/02/18	13:56:45	14:07:12	0' 2"	512		
27	Dhawal Bridge 2 Abutment A2	[N5] Torsion at A MAS5v	SSR-PSEUDO	26/02/18	13:42:11	13:51:41	0' 2"	512		
28	Dhawal Bridge 2 Abutment A2	[N5] Torsion at B MAS5v	SSR-PSEUDO	26/02/18	13:56:45	14:07:12	0' 2"	512		
29	Dhawal Bridge 2 Abutment A2	[C2] Torsion at A MAS5v	SSR-PSEUDO	26/02/18	13:42:11	13:51:41	0' 2"	512		
30	Dhawal Bridge 2 Abutment A2	[C2] Torsion at B MAS5v	SSR-PSEUDO	26/02/18	13:56:45	14:07:12	0' 2"	512		
31	Dhawal Bridge 2 Abutment A2	Torsion at A MAS5v	TE3GCM49-17	26/02/18	13:42:11	13:51:41	9' 24"	19C		
32	Dhawal Bridge 2 Abutment A2	Torsion at B MAS5v	TE3GCM49-17	26/02/18	13:56:45	14:07:12	10' 24"	19C		
33	Donal Bridge Abutment A2	[E]V1 Torsion at A MAS5v	SSR-PSEUDO	26/02/18	17:16:08	17:31:42	0' 2"	512		
34	Donal Bridge Abutment A2	[E]V1 Torsion at B MAS5v	SSR-PSEUDO	26/02/18	17:41:55	18:00:30	0' 2"	512		
35	Donal Bridge Abutment A2	[N5] Torsion at A MAS5v	SSR-PSEUDO	26/02/18	17:16:08	17:31:42	0' 2"	512		
36	Donal Bridge Abutment A2	[N5] Torsion at B MAS5v	SSR-PSEUDO	26/02/18	17:41:55	18:00:30	0' 2"	512		
37	Donal Bridge Abutment A2	[C2] Torsion at A MAS5v	SSR-PSEUDO	26/02/18	17:16:08	17:31:42	0' 2"	512		

Fig. no. 9(a) Recorded data signal

- Polygon selection

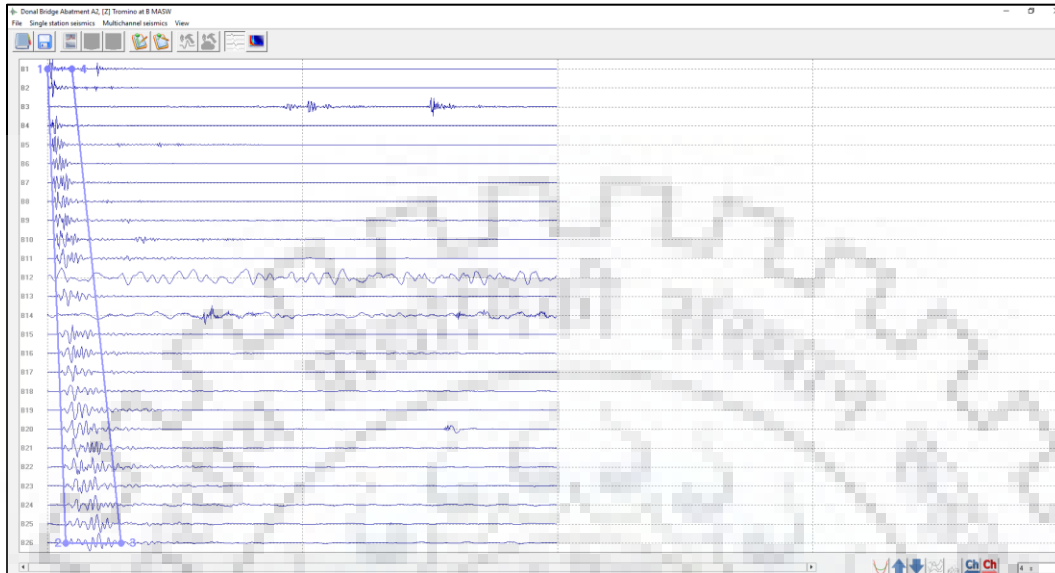


Fig. no.9 (b) Polygon selection for the recorded signal

- Setting the parameters

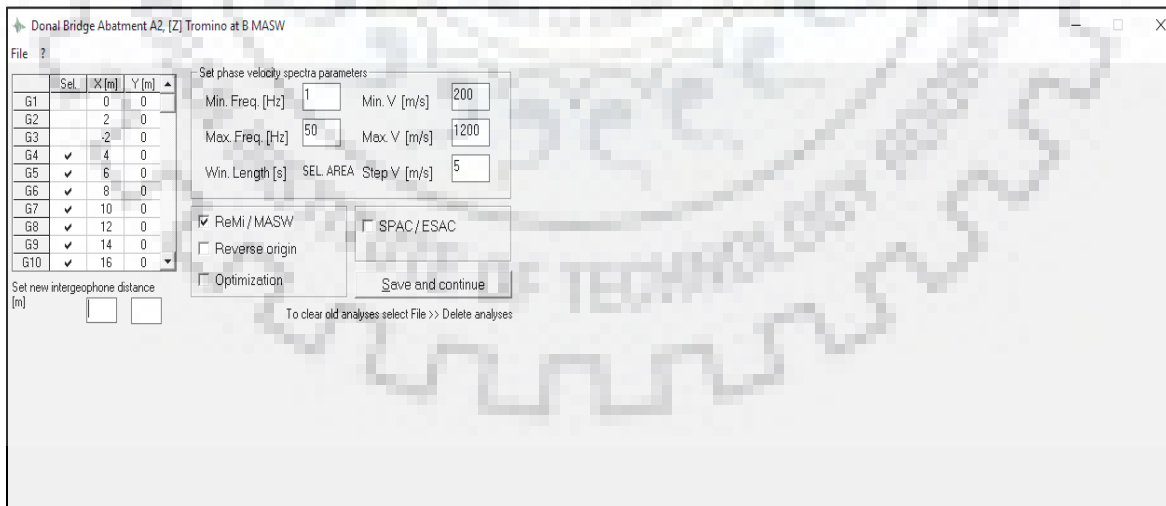


Fig. no. 9(c) setting up the parameters

- Generating the dispersion curve

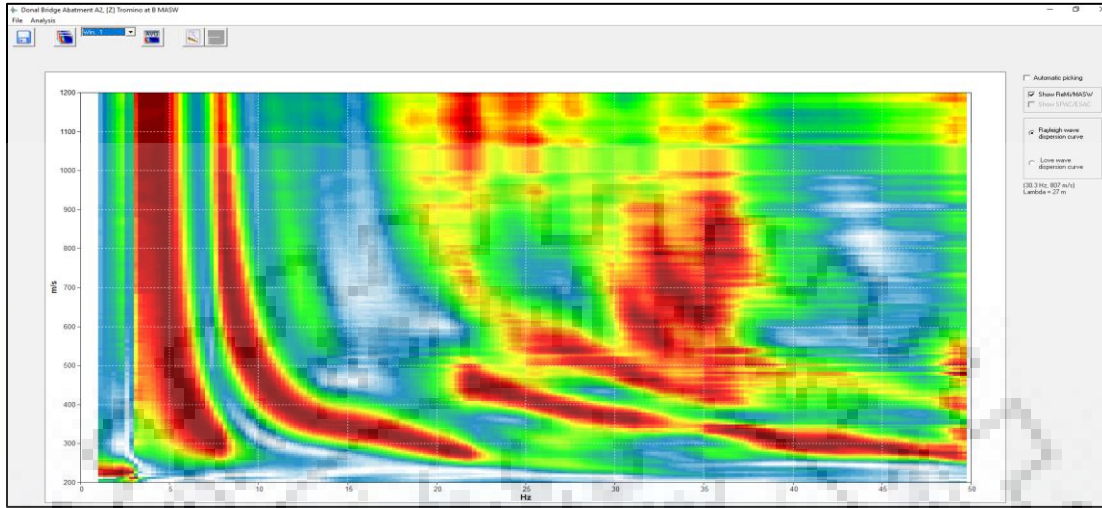


Fig.no.9(d) velocity spectrum for the Donal site

- Forward modeling of dispersion curve

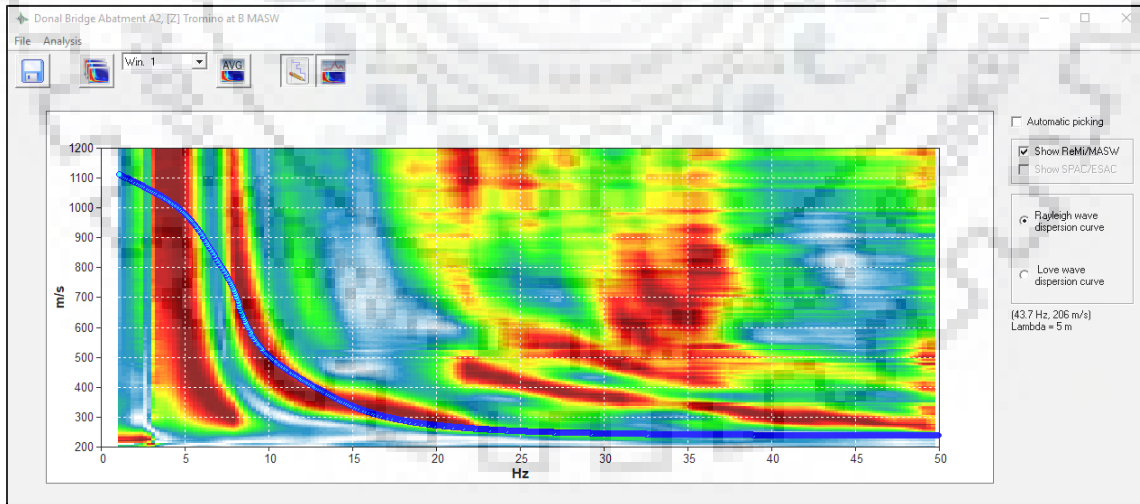


Fig. no. 10(a) extracted dispersion curve after forward model obtained

Table 3: Subsoil model for Donal Khad

Thickness(m)	Vp(m/s)	Vs(m/s)	Poisson's Ratio	Density(t/m <sup>3</sup> )
1.25	539	200	0.42	2.7
10	890	330	0.42	2.7
25	2587	780	0.42	1.7
4	2985	900	0.42	1.9
0	2376	970	0.42	1.9

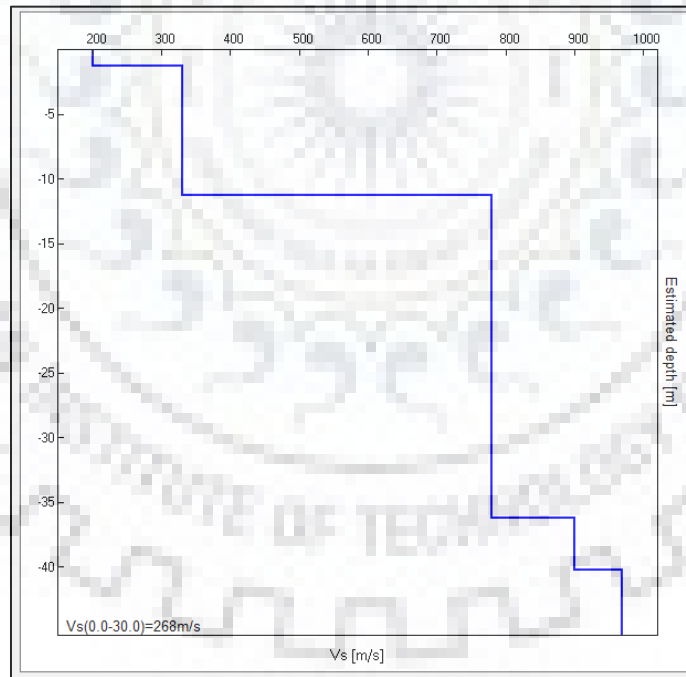


Fig. no. 10(b) velocity depth model for Donal Khad

Similar steps are followed for the site Balaknath Temple and final processing is carried out.

## Chapter 5: Results

Once the data has been processed starting with the acquisition of the multichannel data and ending at the forward modeling of the obtained dispersion curve, one can proceed with analyzing the results from interpretation point of view. Identifying the underlying layers in the subsoil and hence the velocity variation with these layers.

Site1: Donal Khad

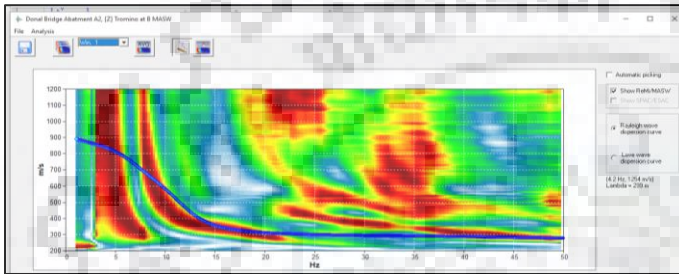


Fig. 11(a) extracted dispersion curve in single mode for Rayleigh Wave - Donal

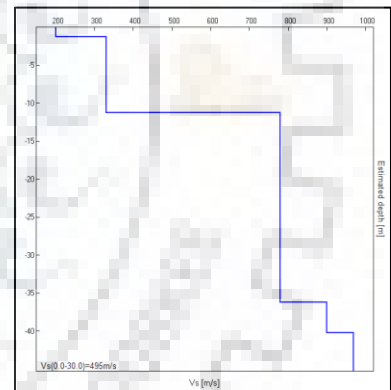
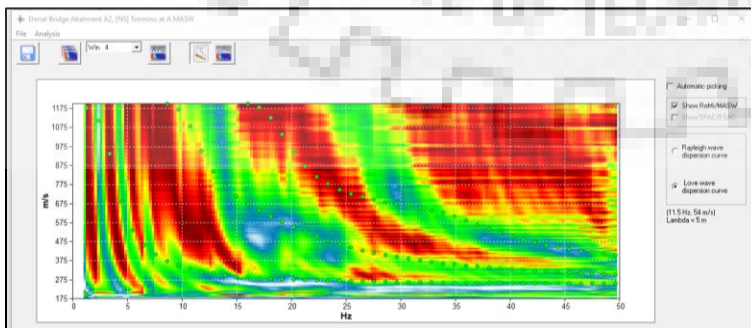


Fig. no. 11(c) Velocity model for Donal





## Site 2: Balaknath Temple

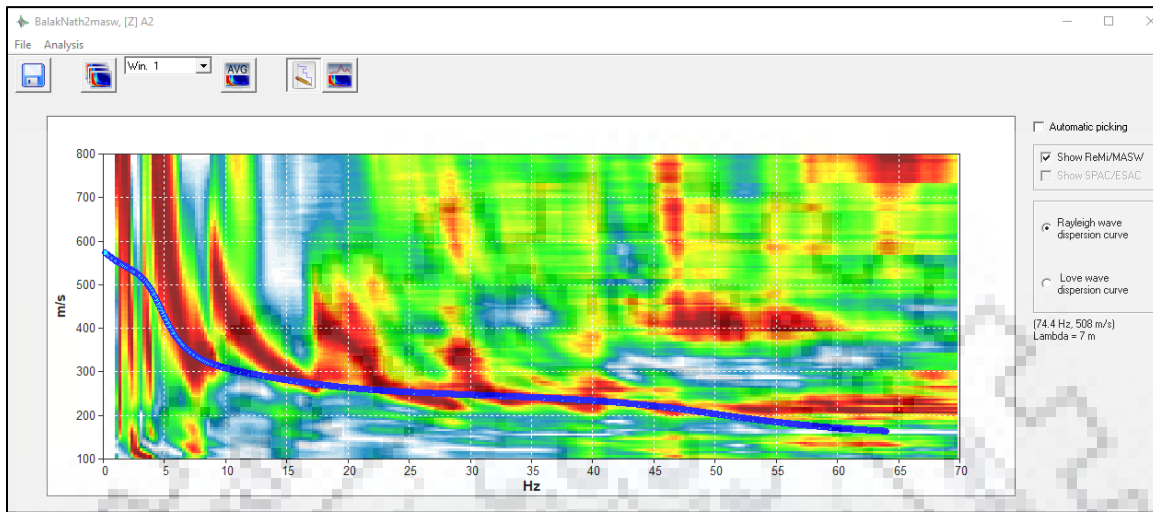


Fig. no. 12(a) extracted single mode dispersion curve for Rayleigh waves for Balaknath Temple

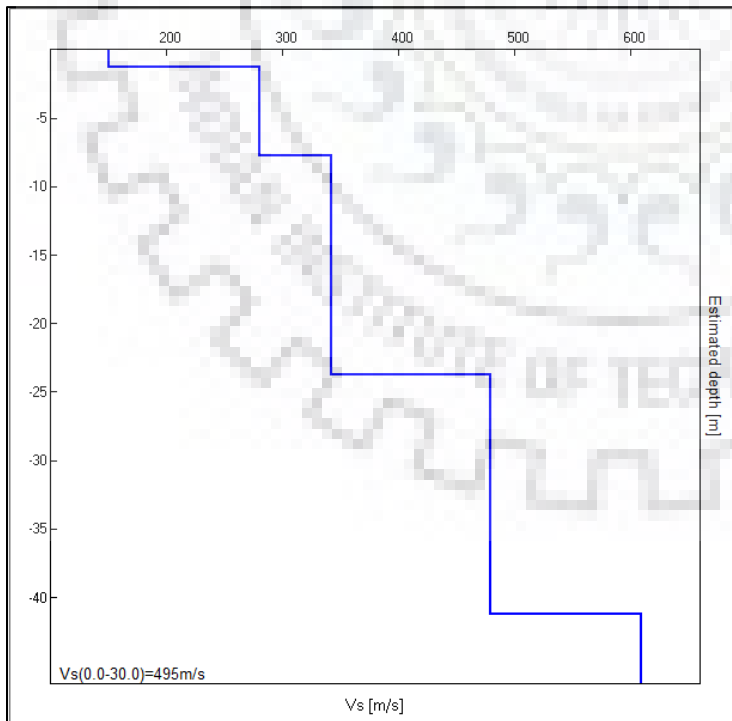


Fig.no.12(b) Velocity model for Balaknath Temple

The results obtained after the final processing of the data are:

At the first site: Donal Khad , the extracted dispersion curve for the Rayleigh waves using the vertical component (z component) of the recorded data fig. no.11(a) is obtained by forward modeling the velocity spectrum and a final velocity-depth model is obtained fig. no. 11(b). Further the velocity depth model verification is carried out by using the Love wave multi- mode dispersion curve which satisfies the model. A total of 3 distinct interval velocities for respective depths can be identified and are present up to depth of 30 m. The value for the  $V_s(0.0-30) = 448$  m/s.

For the site 2: BalakNath Temple, vertical component (z component) of the data is processed and single mode dispersion curve Rayleigh waves fig. no.12(a) is extracted using the forward modeling of the velocity spectrum and the velocity-depth model is obtained fig. no. 12(b). At this site also a total of 3 distinct interval velocities for respective depths can be identified and are present up to depth of 30 m. The value for the  $V_s(0.0-30) = 495$  m/s.

## Chapter 6: Conclusion

---

The estimation of the in-situ shear wave velocity is carried out using various geophysical and other engineering techniques and methods. In this project, Multichannel analysis of the subsurface waves has been used.

There are various variable subsurface properties which influences most subsoil properties in response to the tremor produced by the earthquake ground motion. The major subsoil parameters that hold a direct relationship with measureable parameter are stiffness of the soil, subsoil amplification ability and liquefaction. These parameters are directly related to the maximum capacity of the geotechnical structures they can especially in those regions which are seismically active zones and also used to map the geology of the subsurface structures.

The data acquisition part was carried out using Tromino and wireless trigger at two proposed sites. The processing part is done in the Grilla software which comes as a processing package with Tromino. The processing part is done as follows:

Loading the data into Grilla software, selecting the polygon of data signal, generating the velocity spectrum and finally forward modeling the velocity spectrum to obtain the extracted dispersion curve.

The results obtained at site1: Donal Khad , a total of 3 distinct interval velocities for respective depths can be identified and are present up to depth of 30 m. The value for the  $V_s(0.0-30) = 448$  m/s and for the site2: Balaknath Temple also 3 distinct interval velocities for respective depths can be identified and are present up to depth of 30 m. The value for the  $V_s(0.0-30) = 495$  m/s .

## Chapter 7: References

---

- Ahmed Ismail, F. Brett Denny, Mohamed Metwaly, 2014, Comparing continuous profiles from MASW and shear-wave reflection seismic methods: *Journal of Applied Geophysics* 105 (2014) 67–77
- Aki, K. (1965). A note on the use of microseismics in determining the shallow structures of the Earth's crust: *Geophysics, Vol 30*, 665-666
- Aki, K., and Richards, P.G. (1980). *Quantitative Seismology-Theory and Methods*, Vol.1 and 2, Freeman Company, San Fransisco, 932p.
- Bullen, K.E. (1963). *An introduction to the theory of Seismology: Cambridge Univ. Press.*
- Castellaro, S., and F. Mulargia, 2009b, the effect of velocity inversions on H/V: *Pure and Applied Geophysics*, 166, 567–592, doi: 10.1007/s00024-009-0474-5.
- Castellaro, S., and F. Mulargia, 2014, Simplified seismic soil classification: The VfZ matrix: *Bulletin of Earthquake Engineering*, 12, 735–754, doi: 10.1007/s10518-013-9543-3.
- Chih-Ping Lin, Cheng-Chou Chang, Tzong-Sheng Chang, 2004, The use of MASW method in the assessment of soil liquefaction potential: *Soil Dynamics and Earthquake Engineering* 24 (2004) 689–698
- Foti, S., 2000, Multi-station methods for geotechnical characterization using surface waves: PhDthesis, Politecnico di Torino, Italy.
- Gabriels, P., Snider, R., and Nolet, G., 1987, In situ measurements of shear-wave velocity in sediments with higher-mode Rayleigh waves: *Geophys. Prospecting*, 35, 187-196.
- Grace Nortey, Thomas K. Armah, Paulina Amponsah, 2018, Vs30 mapping at selected sites within the Greater Accra Metropolitan Area: *Journal of African Earth Sciences* 142 (2018)
- Haskell, N. A. 1953, the dispersion of surface waves on multi-layered media, *Bull. Seismological Soc. of Am.*, v. 43, n. 1, p. 17-34.

- Miller, R.D., Xia, J., Park, C.B., and Ivanov, J., 1999, Multichannel analysis of surface waves to map bedrock, *The Leading Edge*, **18**, no. 12, 1392-1396.
- Narayan Roy, Ravi S. Jakka, 2017, Near-field effects on site characterization using MASW technique, *Soil Dynamics and Earthquake Engineering* 97 (2017) 289–303
- Nazarian, S., Stokoe II, K.H., and Hudson, W.R., 1983, Use of spectral analysis of surface waves method for determination of moduli and thickness of pavement systems: *Transportation Research Record No. 930*, 38-45.
- Park, C. B., Ivanov, J., Miller, R. D., Xia, J., and Ryden, N., 2001a, Multichannel analysis of surface waves (MASW) for pavement: Feasibility test: 5th SEGJ Int. Symposium, Tokyo, Japan, January 24-26, 2001
- Park, C.B., Miller, R.D., and Xia, J., 1998, Imaging dispersion curves of surface waves on multi-channel record: [*Expanded Abstract*]: *Soc. Explor. Geophysics*. 1377-1380.
- Park, C.B., Miller, R.D., and Xia, J., 1999, Multi-channel analysis of surface waves (MASW): *Geophysics*, v. 64, no. 3, p. 800-808.